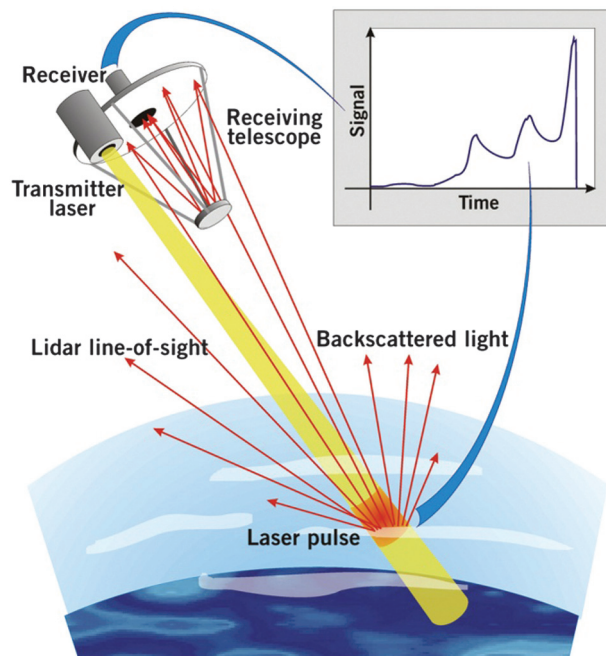
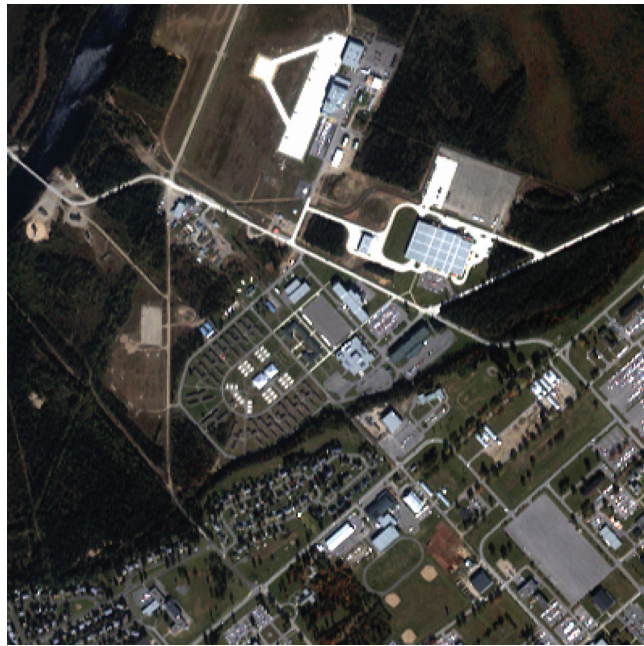


# Color Plates



**Plate 1** A schematic view of the operational concept of a spaceborne lidar (credit: ESA).



**Plate 2** The RGB image of the CFB-site multispectral dataset (reprinted from Ref. 81).



(a) Original multispectral RGB image (4 m)



(b) Pan image (1 m)



(c) Fused image using CRT



(d) Fused image using wavelet transform



(e) Fused image using FRIT



(f) Fused image using PCA

**Plate 3** Fused images in a small region (CFB airport) of the multispectral datacube fused with a real panchromatic image using the CRT, wavelet transform, FRIT, and PCA fusion methods (reprinted from Ref. 81).

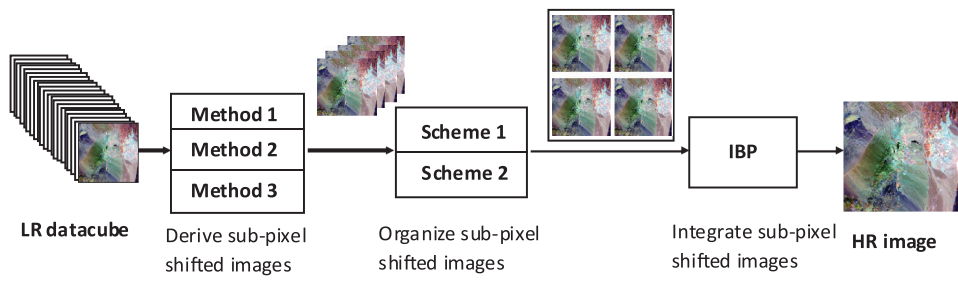


**Plate 4** Block diagram of generating the single-band HR image by exploiting the keystone (reprinted from Ref. 6).

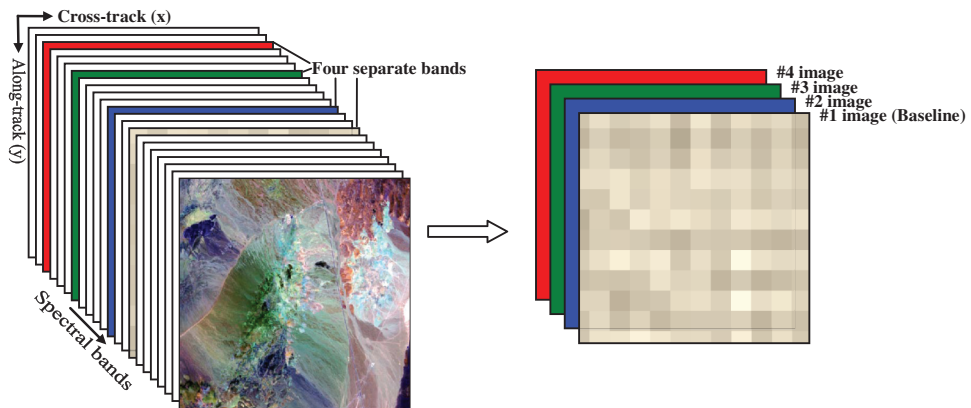


**Plate 5** Four spectral band images extracted from a datacube to be enhanced based on KS-induced subpixel shift related to the baseline image (reprinted from Ref. 6).

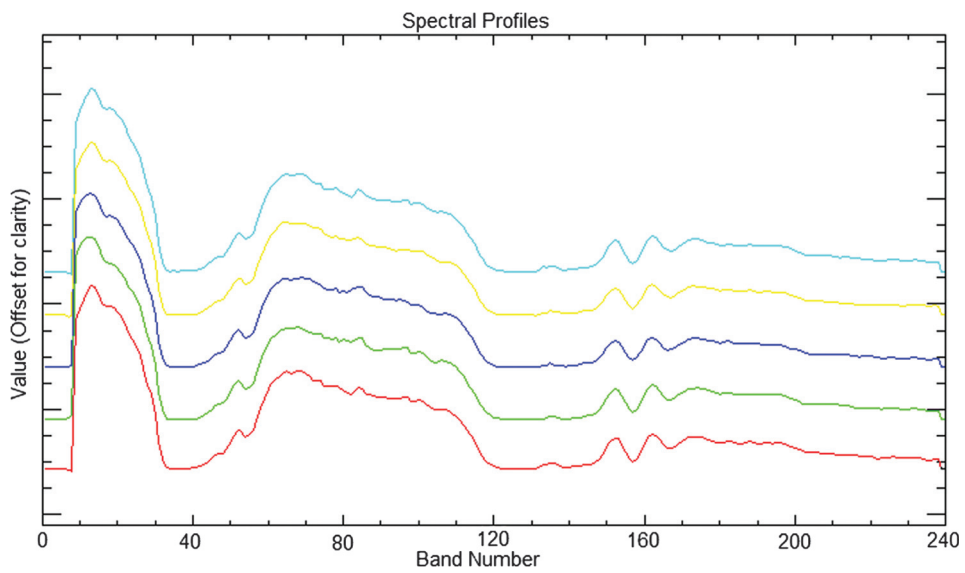


**Plate 6** An example of spectral curve of the awning material (red) extracted from the original datacube and spectral curves of the  $2 \times 2$  pixels in the HR grid (green, blue, yellow, and light blue) extracted from the Target datacube after spatial resolution enhancement using the CRT (reprinted from Ref. 6).

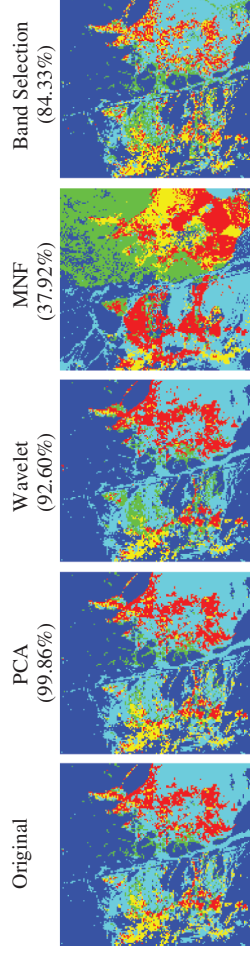


**Plate 7** Classification maps produced from the original Cuprite datacube and the datacubes after DR using the PCA, wavelet, MNF, and band-selection methods, respectively. Twenty-two DR output channels are used. The correct classification rates of the three DR methods with respect to the classification map of the original datacube are also shown (reprinted from Ref. 8).

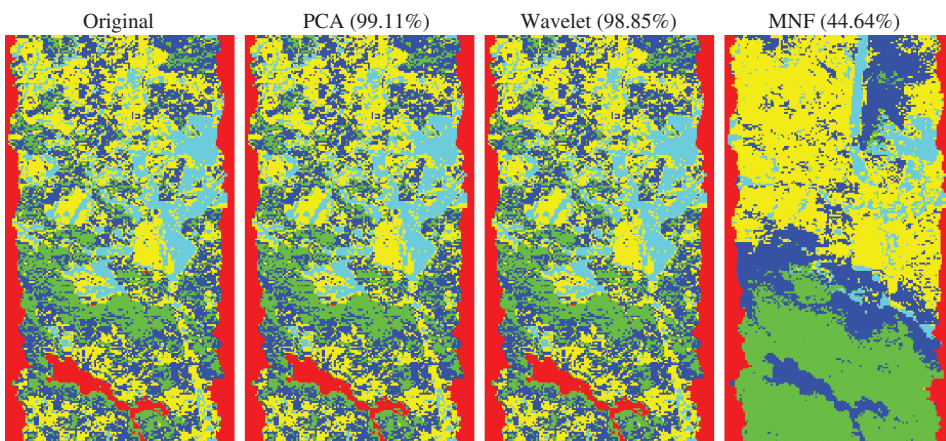


**Plate 8** Maps of unsupervised classification using *k*-means. The first ten output channels are used after dimensionality reduction with the three methods (PCA, wavelet, and MNF). The correct classification rates of the three dimensionality reduction methods with respect to the classification map of the original datacube are also shown (reprinted from Ref. 8).



# Index

- 2D detector array, 205
- 3D VQ, 87
- 6S, 194
  
- A**
- a posteriori* probability, 167
- a priori* knowledge, 56, 167
- à trous*, 251, 255, 275
- absolute calibration, 181
- absolute calibration coefficient, 183
- absorption, 183
- absorption feature, 328
- abundance, 456
- abundance non-negativity, 462
- abundance sum-less-or-equal-to-one, 462
- abundance sum-to-one, 462
- abundance vector, 465
- AC coefficients, 94, 111, 112
- acousto-optical tunable filter (AOTF), 16
- acquisition system, 55
- across-track dimension, 210
- active sensors, 2, 274
- adaptive entropy coder, 107
- additional information, 294
- additive noise, 75, 329
- additive white Gaussian noise (AWGN), 147
- Advanced Land Imager (ALI), 7, 9, 195, 266
- Advanced Land-Observing Satellite (ALOS), 3, 278
- advanced orbiting systems (AOSs), 126
- Advanced Responsive Tactically Effective Military Imaging Spectrometer (ARTEMIS), 19, 23
- Advanced Visible and Near-Infrared Radiometer (AVNIR), 10
- aerobraking, 22
- aerosol, 31, 32
- aerosol and water droplets, 35
- aerosol optical properties, 96
- affine transform, 276
- agriculture, 182
- air pollution, 27
- Airborne Visible/Infrared Imaging Spectrometer (AVIRIS), 16, 87, 188, 205, 216, 233, 332, 419, 439, 470
- airport, 269
- along-track, 7, 12, 15, 17, 18, 38, 314, 332
- alphabet, 151
- alunite, 422
- amplifier, 84
- analog-to-digital converter, 84
- analysis high-pass filter, 98
- ancillary channel, 70
- ancillary data, 46, 130, 134
- ancillary products, 43
- angular resolution, 265
- anisotropic diffusion, 75
- antishifted, 264

- aperture, 327  
apoapsis, 36  
application-specific integrated circuit (ASIC), 93  
Aqua satellite, 34, 98  
archaeology, 31  
archived data, 45  
arithmetic coding, 101  
arithmetic combination fusion, 246  
arithmetic mean, 105  
ARSIS, 246, 255  
artificial site, 193  
assessment, 379  
assumption, 148  
asymptote, 148  
at-sensor brightness temperature, 197  
at-sensor radiance, 195, 332  
atmosphere, 84, 183  
atmosphere absorption transmission spectra, 212  
atmospheric absorption lines, 212  
Atmospheric Chemistry Experiment–Fourier Transform Spectrometer (ACE-FTS), 28  
atmospheric conditions, 253, 292  
atmospheric correction, 84  
Atmospheric Dynamics Mission Aeolus (ADM-Aeolus), 35  
Atmospheric Infrared Sounder (AIRS), 98, 117, 98  
Atmospheric Laser Doppler Lidar Instrument (ALADIN), 35  
atmospheric parameter, 181  
atmospheric scattering, 455  
atmospheric temperature, 27, 96  
atmospheric transmissivity, 32  
audio data, 126  
Aura satellite, 27, 34  
Aurora satellite, 233  
automated morphological endmember extraction (AMEE), 458, 463  
automatic target generation process (ATGP), 459, 463  
avalanche photodiode (APD), 34, 38  
awning, 305, 381, 392
- B**  
back-projection, 264, 302  
background, 95  
background masks, 392  
band-center wavelength, 216  
band correlation minimization (BCM), 422  
band dependence minimization (BDM), 422  
band-pass filter, 14  
band ratio fusion, 246  
band reordering, 82  
baseline image, 296, 309  
Bayesian estimation, 328  
BayesShrink threshold, 330  
beam splitter, 23, 26  
belief propagation (BP), 172  
bench test, 130  
Bernoulli–Gaussian model, 328  
Besov ball projections (BBPs), 343  
bias, 277  
bias-adjusted reordering, 98  
bicubic interpolation, 307  
bidirectional reflectance distribution function (BRDF), 20, 183  
bilinear interpolation, 71, 264, 303  
binary phase shift keying (BPSK), 158  
biorthogonal filter, 93  
biorthogonal wavelet, 255  
birefringence, 16  
bit-error rate (BER), 146, 147  
bit signal-to-noise ratio (bit-SNR), 147, 169  
bitplane encoder (BPE), 93, 110  
bitrate, 93

- bits per pixel per band (bpppb), 117
- bitstream, 83, 157
- bivariate wavelet shrinkage, 362, 440
- bivariate wavelet shrinkage and PCA (BWS+PCA) method, 440
- bivariate wavelet thresholding, 350, 352, 442
- blackbody, 187, 188, 191
- blind distortion measurement, 74
- block-adaptive entropy encoder, 117
- block length, 151
- block-matching and 3D filtering (BM3D), 358, 362
- block size, 147
- blocking, 74
- blocking artifact 75
- Blu-ray discs, 151
- Blue Books, 107
- blurring, 74
- blurring function, 302
- Bose–Chaudhuri–Hocquenghem (BCH) codes, 151
- boundary, 421
- boundary conditions, 116
- bounded distance, 156
- bright target scene, 193
- brightness, 247
- brightness temperature, 98
- broadband indices, 365
- Brovey transform, 246, 252, 257
- buddingtonite, 422
- building roof, 272
- buried mines, 380
- byte, 130
  
- C**
- C-band, 278
- cadmium-zinc-telluride (CZT), 39
- calcite, 422
- calibration, 179
- calibration and validation, 197
- calibration lamp, 179
- Canadian Force Base (CFB), 268
- Canadian Hyperspectral Environment and Resource Observer (HERO), 291, 332
- canopy, 365
- carbon compounds, 51
- carbon-containing species, 53
- carbon monoxide, 27
- carbon sensor, 52
- carbonates, 22
- Cassini, 169
- CCSDS 121.0-B, 107
- CCSDS 122.0-B, 110
- CCSDS 123.0-B, 114
- CCSDS File Delivery Protocol (CFDP), 127
- ceiling function, 104
- celestial bodies, 1
- central local difference, 117
- Chandrayaan, 22
- channel coding layer, 129, 145
- channel noise, 146
- characterization, 180, 183
- charge-coupled device (CCD), 4, 6, 10, 13, 20
- chi-square, 368
- China–Brazil Earth Resources Satellites (CBERS), 10
- chlorophyll, 364
- chromatic aberration, 208, 292
- circulant, 172
- civilian, 1
- classic keystone, 235, 294
- classification, 419
- classification map, 426, 428
- climate change, 27, 49
- clockwise rotation, 238
- closeness of pixel intensity, 299
- closest vertex, 467

- Cloud-Aerosol Lidar and Infrared Pathfinder Satellite Observations (CALIPSO), 34
- Cloud-Aerosol Lidar with Orthogonal Polarization (CALIOP), 34
- cloud cover, 51
- cloud detection, 95
- cloud-free, 194
- cloud optical properties, 96
- cloud-top height, 51
- CloudSat, 34
- cluster, 85
- cluster index, 86
- cluster SAMVQ, 84
- co-registration, 23, 244, 276
- coating thickness, 15
- codeblock, 141, 148
- codebook, 85, 100
- codebook generation, 85, 87
- codebook training, 85
- coded dataset, 109
- codevector, 86
- codevector matching, 85, 87
- codeword, 100, 148, 167
- coding gain, 105
- coding time, 87
- coherent regularity, 329
- Coiflets, 343
- color distortion, 246
- color fusion, 246
- column-oriented local sum, 116
- combination, 243
- command data, 43
- Committee on Earth Observation Satellites (CEOS), 197
- common geometric base, 291
- common radiometric framework, 292
- communications headers, 46
- communications satellites, 1
- Compact High-Resolution Imaging Spectrometer (CHRIS), 19, 20
- Compact Reconnaissance Imaging Spectrometer for Mars (CRISM), 19, 21
- compact support, 96, 343
- compactness, 328
- compatibility, 128
- complementary part, 421
- complex ridgelet coefficient, 313
- complex ridgelet transform (CRT), 261, 265, 313
- complexity, 289
- compressed data, 83
- compression engine (CE), 89
- compression error, 84
- compression ratio (CR), 81, 90
- computational complexity, 87, 354, 429, 459
- concatenated code, 149
- constraint energy minimization, 425
- context-adaptive nonlinear prediction, 97
- context-based adaptive arithmetic coder, 101
- continuum term, 262
- contour plots, 234
- contrast, 392
- contrast enhancement, 68, 311
- control center, 44
- conventional full-reference metrics, 57
- convergence, 295
- convex cone analysis (CCA), 458
- convex set, 419
- convexity, 101
- convolution operator, 303
- convolutional code (CC), 129, 147, 157
- convolutional inner code, 129, 164
- correcting capability, 157
- correlation coefficient, 59, 240, 249, 277

- correlation similarity measure (CSM), 368
  - correlation vector quantization (CVQ), 87
  - cosine, 328
  - cosine effect, 197
  - cotton, 305, 381, 392
  - covariance matrix, 352, 421, 420
  - coverage area, 392
  - cross-calibration, 193
  - cross-support, 107, 125, 145
  - cross-talk, 15
  - cross-track, 12, 17, 38, 314, 332
  - cross-track footprint, 95
  - Cross-track Infrared Sounder (CrIS), 27
  - cross-track line, 205, 217, 332
  - cubic convolution, 258
  - Cuprite, 71, 267, 355, 361
  - current spectral band, 115
  - curve fitting, 366
  - cutoff frequency, 341
  - cyclic, 150
- D**
- dark current, 84
  - dark leakage current, 84
  - dark target scene, 193
  - data archive, 44
  - data capture, 44
  - data compression, 56
  - Data Compression Working Group (DCWG), 106
  - data-driven threshold, 330
  - data handling, 127
  - data holdings, 45
  - Data Information System, 45
  - data link protocol, 127
  - data product levels, 43, 45
  - data products, 55
  - data volume, 56
  - datacube, 57
  - Daubechies, 343
  - DC coefficient, 94, 111, 112
  - de-elevate noise level, 337
  - de-shifting, 303
  - deblurring, 295
  - decimation operation, 264
  - decision-level fusion, 245
  - decision rules, 245
  - decoder, 86
  - deep-space channel, 149
  - deep-space-network monitor files, 48
  - degradation, 190, 193, 340
  - deinterleaving, 154
  - denoised signal, 330
  - denoising, 330
  - Department of Defence (DoD), 18
  - depunctured, 160
  - derived products, 55
  - derived target, 393
  - despeckled SAR image, 275
  - detectability, 383
  - detector array, 84
  - detector elements, 12
  - detector nonlinearity, 183
  - deviation index (DI), 249
  - diagonal linear projection (DLP), 331
  - diagonal linear shrinker (DLS), 331
  - diagonal matrix, 102
  - dichroic filter, 20
  - difference in variance (DIV), 278
  - differential pulse code modulation (DPCM), 91
  - digital count, 84, 181
  - digital denoising, 327
  - digital number (DN), 184
  - digital surface model (DSM), 4
  - dilation operation, 463
  - dimensionality, 352
  - dimensionality reduction, 419, 459
  - diode-laser-pumped, 34, 35
  - diode-pumped, 32, 33
  - Dirac distribution, 262

- direct-detection Doppler wind lidar, 35  
 directional local differences, 116–117  
 discrete cosine transform (DCT), 75, 82, 92  
 discrete projection-slice theorem, 262  
 discrete shift increment, 215  
 discrete wavelet transform (DWT), 255, 330  
 discrimination capability, 62  
 dispersing element, 12, 13, 16, 55  
 dispersing-element-based sensor, 15  
 dissimilar pixel, 463  
 dissimilarity CSM, 369  
 dissimilarity MSAM, 369  
 dissimilarity XSM, 369  
 distance-based indices, 365  
 distance measure, 468  
 distinctive pixel, 459, 463  
 distortion channel, 67  
 distortion measures, 56  
 distortion types, 74  
 distributed active archive centers (DAACs), 43  
 downlinking bandwidth, 56  
 downsampling, 70, 268, 421, 448  
 downsampling operator, 302  
 dual basis, 154  
 dual-tree complex wavelet transform (DTCWT), 261, 313, 350, 353  
 duplicate data, 46  
 dynamic range, 196, 297
- E**
- Earth–atmosphere system, 185  
 Earth-fixed reference grid, 50  
 Earth-observation satellites, 1  
 Earth Observer-1, (EO-1), 7, 9, 18, 19, 40  
 Earth Observing System (EOS), 43  
 Earth–Sun distance, 197  
 Earth year, 36  
 Earth’s magnetic field, 1  
 echo pulse, 36  
 edge detection, 232  
 effective radiance, 185  
 effectiveness, 289, 379  
 effects of pollution, 1  
 eigenpairs, 432  
 eigenvalue, 352, 420, 431  
 electromagnetic energy, 179, 274  
 electromagnetic spectrum, 11, 187, 364  
 electronically tunable filter (ETF), 14, 15  
 elevated noise level, 337  
 embedded block coding with optimized truncation, 97  
 embedded zerotree wavelet (EZW), 96  
 emissivity, 96  
 encapsulation, 128  
 endmember, 380, 419, 455  
 endmember extraction, 419, 422  
 endmember spectrum, 380  
 energy compaction, 105  
 energy flows, 1  
 energy shifting, 75  
 engineering data, 47, 125  
 engineering demonstration unit (EDU), 29  
 engineering sensors, 145  
 engineering telemetry, 43  
 Enhanced Thematic Mapper Plus (ETM+), 8, 191  
 Enhancing Spatial Resolution (ESR), 291  
 entrance pupil, 183, 184  
 entrance slit, 189  
 entropy, 82, 249, 433  
 entropy encoder, 83, 101, 114

- Environment for Visualizing Images (ENVI), 307, 428, 434, 458  
Environmental Mapping and Analysis (EnMAP), 19, 23  
ENVISAT, 19  
equivalent radiance, 185  
erasure code, 150  
ERGAS, 61, 272, 317  
ergodic, 328  
erosion operation, 463  
erroneous symbol, 150  
error containment, 93  
error-correcting capability, 154  
error-correcting code, 157  
error floor, 170  
error-free channel, 148  
error measurement, 57  
error-prone, 167  
error rate, 147  
error-resistant, 167  
errors-and-erasures, 155  
Euclidean distance (ED), 87, 469  
Euclidean distance-modified, 469  
European Organization for the Exploitation of Meteorological Satellites (EUMETSAT), 26  
even filter, 265  
exclusive-or gate, 159  
exhaustive search, 476  
exoatmospheric irradiance, 212  
experiment data records, 46  
exposure, 84
- F**  
Fabry–Pérot (F-P) filter, 16  
factorial kriging, 380  
false alarm, 380  
false alarm probability, 470  
false positive, 379  
false positive rate (FPR), 389  
far-infrared (FIR), 5  
farmland, 272  
fast Fourier transform (FFT), 75, 262  
fast iterative pixel purity index (FIPPI), 462  
fast N-FINDR (FN-FINDR), 465  
fast precomputed vector quantization (FPVQ), 99  
feature extraction, 70  
feature-level fusion, 244  
featureless, 255  
feedback, 166  
fiber optic bundle, 191  
fidelity mode, 90  
fidelity threshold, 85  
field-motion compensation, 27  
field of view (FOV), 3, 455  
fingerprints, 11  
finite ridgelet transform (FRIT), 261  
first header pointer, 138  
first-in-first-out (FIFO), 92  
fit curve, 218  
fixed-length coding, 91  
fixed-length frame, 126  
fixed-variance additive noise, 329  
fixed-variance noise, 329  
Fizeau spectrometer, 35  
flatter amplitude, 310  
floating-point DWT, 110  
flooring function, 104  
fluctuation, 222  
fluorescence, 31  
focal plane, 12  
focal plane array, 23  
focusing optics, 12  
foliage, 275  
foreground, 95  
forest chemistry, 354  
forest fires, 51  
forest health, 354  
formulation, 183  
forward error correcting code, 154  
Fourier domain, 262

- Fourier transform domain, 328
- Fourier Transform Hyperspectral Imager (FTHSI), 28
- Fourier transform spectrometer (FTS), 23, 81
- Fourier transform spectroscopy, 2
- fraction, 392, 456
- fraction image, 392
- fractional map, 462
- frame-based image format, 107
- frame count, 128
- frame data field, 128
- frame-error control field, 141
- frame-error rate, 147
- frame identification, 128
- Fraunhofer lines, 212
- free distance, 157
- free-flying satellite, 32
- frequencies, 328
- frequency domain, 75
- frequency domain reconstruction, 295
- frequency space, 262
- frown, 205
- full-prediction mode, 117
- full-reference metrics, 56, 57
- full search, 88
- full width at half maximum (FWHM), 15, 16, 216
- fully constrained least-squares linear unmixing, 459, 464
- fully constrained spectral unmixing, 462
- fusion, 76
- G**
- gamma function, 73
- Gaussian blurs, 75
- Gaussian channel, 149
- Gaussian distribution, 99
- Gaussian model, 328
- Gaussian spectral response profile, 219
- generalized Gaussian, 72
- generalized Lloyd algorithm (GLA), 87
- geocoded, 244
- geolocated radiances, 50
- geopositioning, 1
- georeferencing, 46
- geographical information systems, 243
- geological site, 332
- geometric approach, 458
- geometric calibration, 46
- geometric distortion, 208, 292
- geometric mean, 105
- geometric mixture model, 456
- geometric registration, 291
- geomorphology, 31
- geophysical imaging, 262
- geophysical information, 244
- geophysical products, 50
- Geoscience Laser Altimeter System (GLAS), 34
- Geosynchronous Imaging Fourier Transform Spectrometer (GIFTS), 29, 95
- geosynchronous orbit, 29, 95
- ghosting, 183
- gigabit (Gb), 9
- glass index, 15
- global blur, 75
- global maximum, 476
- global sea level, 34
- global threshold, 330
- global warming, 27
- GPS coordinate, 244
- granule, 98
- grass, 305
- grating, 12, 13, 18
- grating prism, 14
- gray-level, 75
- Greater Victoria Watershed District (GVWD), 332, 355, 361



greatest lower bound, 330  
green felt, 305  
grism, 13, 14  
ground-echo pulses, 38  
ground footprint, 455  
ground footprint size, 2, 3, 7, 10, 18  
ground moisture condition, 253  
ground reception station, 44  
ground reference scene, 179  
ground sample, 205  
ground sample cell, 12  
ground sample distance (GSD), 20  
ground spectra, 394  
ground station, 126  
ground swath, 289  
ground-to-space link, 126  
ground truth, 379, 392, 423, 435  
ground velocity, 38  
guideline, 130

## H

Hamming distance, 87, 157  
hard-decision code, 157, 161  
hard thresholding, 441  
hardware implementation, 89  
harmony, 125, 145  
header, 93  
heavyweight, 32  
helicopter, 269  
heterogeneous, 455  
heuristic approach, 458  
HFC method, 470  
HH-polarized, 278  
hidden targets, 274  
hierarchical self-organizing cluster  
  vector quantization (HSOCVQ), 90  
hierarchical wavelet transform  
  subbands, 96  
high-gain setting, 198  
high-pass filter, 98, 214, 246, 337,  
  421  
high-pass filter bank, 257  
high power, 32

high resolution (HR), 245, 256, 294  
High-Resolution Geometrical  
  (HRG), 91  
High-Resolution Stereoscopic  
  (HRS) imaging instrument, 91  
High-Resolution Visible (HRV), 10  
High-Resolution Visible and  
  Infrared (HRVIR), 10  
high spatial resolution, 291  
histogram, 72  
histogram matching, 256  
homogeneous, 194, 455  
hot spots, 51  
housekeeping, 9, 43, 125  
housekeeping sensors, 145  
Hubble telescope, 29  
human brain, 67  
human color perception, 248  
human visual system (HVS), 67, 68  
hybrid spatial-spectral component,  
  344  
hybrid spatial-spectral noise  
  reduction (HSSNR), 336, 379  
hypercomplex, 62, 65  
Hyperion, 18, 117, 205, 216, 233, 266  
hyperplane, 101  
hyperspace, 458  
hyperspectral, 2, 114  
Hyperspectral Digital Image  
  Collection Experiment  
  (HYDICE), 470  
hyperspectral sensor, 11, 56

## I

Ice, Cloud, and Land Elevation  
  Satellite (ICESat), 34  
ice-sheet mass, 34  
ICER, 114  
identification, 128  
identifier, 109  
identity matrix, 431  
idle, 140  
IKONOS, 61, 246, 277, 305

- illumination, 86, 253, 292
- image-data compression, 107
- Image-Data Compression standard, 127
- image fusion, 243
- image information, 67
- image interpretation, 93
- image quality criteria, 56
- image quality metric, 55, 304
- image transform, 328
- imaging Fourier transform spectrometer (IFTS), 23
- Imaging Infrared Radiometer (IIR), 35
- imaging spectrometer, 11, 292
- Imaging Spectrometer Data Analysis System (ISDAS), 215, 392, 409
- impulsive noise, 84, 149
- in-band planetary albedo, 196
- in-flight calibration, 181
- infimum*, 330
- increased confidence, 245
- independence of errors, 148
- independent component analysis (ICA), 419, 458
- index, 86
- index map, 87
- Indian Micro Satellite, 10
- Indian Space Research Organization (ISRO), 10
- individual bit, 147
- individual codeword, 147
- individual frame, 147
- infinite interleaving, 149
- inflection point, 366
- information amount, 67
- information bit, 152
- information block, 156
- information fusion, 244
- information management, 44
- information symbol, 151, 157
- information volume, 304, 434
- infrared, 2
- Infrared Atmospheric Sounding Interferometer (IASI), 26, 95
- Infrared Multispectral Scanner (IRMSS), 10
- infrared rays, 2
- inner code, 163
- inner convolutional code, 151
- insect invasion, 354
- instantaneous field of view (IFOV), 12, 20, 455
- instrument configuration, 86
- instrument health, 50
- instrument noise, 84
- instrument responsivity, 184
- instrument status, 50
- integer DWT (IDWT), 110
- integer wavelet transform (IWT), 98
- integrating sphere, 184
- integration, 130, 243
- integration error, 339
- integration time, 17, 180, 205
- intensity function, 262
- intensity-hue-saturation (IHS), 246, 258
- intensity image, 246
- intensity modulation, 23, 275
- interagency cross-support, 147
- interband, 65
- interband correlation, 231, 241, 294, 342, 370
- interband spatial misregistration, 233, 292
- interconnection, 130
- interface protocol, 128
- interference filter, 13, 14
- interferogram components, 25
- interferometer-based filters, 16
- interleaving, 154
- interleaving depth, 154
- International Organization for Standardization (ISO), 92, 107, 125

- International Space Station, 126  
international standard, 125  
Internet protocol, 126  
interoperability, 107, 130  
interpolation, 72, 216, 295  
interpretation, 245  
intersection, 311  
intraband, 64  
intrinsic noise, 84  
invariant, 430  
inverse discrete wavelet transform (IDWT), 330  
inverse Gaussian (IG), 366  
irregular LDPC code, 172  
iterated constrained endmembers (ICEs), 458  
iteration, 87  
iterative back-projection (IBP), 71, 264, 295  
iterative deconvolution, 295  
iterative error analysis (IEA), 392, 408, 462
- J**  
Japan Aerospace Exploration Agency (JAXA), 3  
Jet Propulsion Laboratory (JPL), 16  
JPEG, 74, 92  
JPEG-LS, 96, 117  
JPEG2000, 96
- K**  
kaolinite, 422  
Karhunen–Loève transform (KLT), 101  
kernel function, 380  
Key Lake, 71, 219, 267, 305  
keystone (KS), 17, 205, 208, 290, 292  
keystone characteristics, 290  
keystone figure, 294  
keystone-induced spatial shift, 294  
known endmember, 457  
Kullback–Leibler distance, 61, 72
- L**  
L-band, 278  
La Crau, France, 194  
Lake Tahoe, Nevada, 194  
Lambertian, 185  
land-cover type, 455, 456  
land-surface temperature, 51  
lander, 127  
Landsat, 3, 5–8, 39, 42, 91, 194, 246  
Landsat Data Continuity Mission, 9  
landscape, 456  
Laplacian eigenmap, 419, 436  
Laplacian model, 328  
laser altimetry, 31, 37  
laser beams, 38  
laser-illuminated surface, 32  
laser-pulse energy, 36  
laser pulses, 34  
laser transmitter, 33–34  
lattice computing approach, 458  
layering, 127  
leading bit, 140  
leaf area index (LAI), 366  
least upper bound, 330  
lens, 327  
Levinson–Durbin algorithm, 103  
lidar, 2, 30  
Lidar In-space Technology Experiment (LITE), 32  
life on Mars, 52  
lifecycle, 130  
lifting scheme, 96  
lightweight optics, 32  
likelihood, 467  
limb mode, 27  
Linde–Buzo–Gray (LBG) algorithm, 100  
line of blocks, 92  
linear combination, 100, 457, 459  
linear contrast enhancement, 307

- linear correlation coefficient, 380
  - linear detector array, 7, 8, 17, 205, 217
  - linear finite-state machine, 157
  - linear histogram stretching, 307
  - linear mixture model, 456, 459
  - linear spectral mixture, 456
  - linear spectral unmixing (LSU), 455
  - linear variable filter, 14
  - linear-phase filter, 265
  - linearity, 183
  - linearly constrained minimum
    - variance-based constrained band-selection (LCMV-CBS), 422
  - liquid crystal tunable filter (LCTF), 16
  - local difference value, 115
  - local gradient, 97
  - local mean, 277
  - local mean and variance matching (LMVM), 258
  - local mean matching (LMM), 258
  - local spatial window, 432
  - local sum, 115
  - local topological structure, 429
  - local variance, 276
  - locality characteristics, 436
  - locally linear embedding, 419, 429
  - locally linear patch, 430
  - log files, 48
  - long-wave infrared, 9
  - lookup table (LUT), 82, 101
  - lossless compression, 81
  - lossless data compression (LDC), 107
  - Lossless Data Compression
    - standard, 127
  - lossless multispectral &
    - hyperspectral image compression, 107
  - lossless-to-lossy compression, 114
  - lossy compression, 81
  - lossy data compression, 56
  - low Earth orbit (LEO), 18
  - low error probability, 146
  - low-density parity-check (LDPC)
    - code, 147, 171
  - low-energy PCA components, 361
  - low-energy PCA output channel, 350
  - low-gain setting, 198
  - low-order polynomial, 215
  - low-pass filter, 98, 328, 421
  - low-pass filter bank, 257
  - low resolution, 70, 247, 256, 294
  - lower-diagonal-upper, 102
  - lower-dimensional space, 461
  - lower triangular matrix, 102
  - lower-upper decomposition, 467
  - luminance function, 66
  - luminance-weighted norm, 75
  - Lunar Lake and Railroad Valley in Nevada, 194
  - Lunar Orbiter Laser Altimeter (LOLA), 37
  - Lunar Reconnaissance Orbiter (LRO), 37
  - lunar topography, 37
- M**
- M-CALIC algorithm, 85
  - Mahalanobis distance, 380
  - major field, 134
  - mandatory, 130, 131
  - manifold, 430
  - mapped prediction residual, 114
  - mapping, 1, 107
  - Mars Global Surveyor (MGS), 34
  - Mars Orbiter Laser Altimeter (MOLA), 34
  - Mars Pathfinder, 169
  - Mars Reconnaissance Orbiter (MRO), 21
  - Martian carbon chemistry and carbon cycling, 52

- Martian orbit, 21
- mask, 383
- mass memory, 127
- master channel, 136
- matched codevector, 86
- matched filter, 379
- material species, 294
- MATLAB, 432
- maximum absolute difference (MAD), 58, 85, 93
- maximum kernel size, 463
- maximum likelihood, 158, 160
- maximum norm, 460
- maximum reflectance, 366
- maximum spectral angle, 60
- maximum spectral information divergence, 61
- maximum value, 58
- mean absolute error, 59
- mean of spectral vector, 60
- mean sea surface, 32
- mean spectrum, 462
- mean-square error (MSE), 57, 304
- mean-square spectral error (MSSE), 59
- mean SSIM, 67
- median filtering, 307
- medical imaging, 85, 262
- Medium-Resolution Imaging Spectrometer (MERIS), 19, 20
- memory consumption, 429
- memoryless, 154
- mercury-cadmium-telluride (MCT), 23
- Mercury Laser Altimeter (MLA), 36
- Mercury orbit, 36
- Mercury Surface, Space Environment, Geochemistry, and Ranging (MESSENGER), 36
- Mercury years, 36
- merging, 243
- meteorological satellite, 49
- methane, 27
- MetOp satellites, 26
- Michelson interferometer, 23, 26, 28, 96
- microprocessor, 130
- microwave sensors, 2
- Midcourse Space Experiment (MSX), 18
- middle-infrared (MIR), 5
- Mie channel, 35
- Mie lidar, 31
- Mie scattering, 31
- military, 1
- mill complex, 305
- mine complex, 305
- mineral detection, 419
- minimax threshold, 330
- minimum distance, 151, 171
- minimum distance partition, 88
- minimum kernel size, 463
- minimum noise fraction (MNF), 328, 370, 419, 459
- minimum-noise ladder-based structure, 104
- minimum reflectance, 366
- minimum volume-constrained non-negative matrix factorization, 458
- mining lay-down area, 311
- misalignment, 229
- miscompensation, 231
- misregistration, 55, 205
- mission, 126
- mission-data systems, 44
- mixing pixel, 455
- mixture-tuned matched filter, 380
- mode of operation, 50
- modified chlorophyll absorption in reflectance index, 365
- modified IHS, 258
- modified simple ratio, 365
- modified soil-adjusted vegetation index, 365

- modified spectral angle mapper (MSAM), 368  
 modified VIF (MVIF), 305  
 MODTRAN, 194, 212, 215  
 modular optoelectronic multispectral scanner (MOMS), 190  
 modular optoelectronic scanner (MOS), 190  
 modulation, 127  
 modulation transfer function (MTF), 50, 55, 182  
 modulo-2, 141  
 modulo-256, 137  
 moisture, 96  
 moisture content, 275  
 molecular scattering, 35  
 monitoring natural disaster, 182  
 monitoring pond, 311  
 monochromatic components, 12  
 monochromatic image, 206  
 monochromatic spectrum, 16  
 monochromator, 188  
 Moon Mineralogy Mapper (M3), 19, 22  
 morphological eccentricity index (MEI), 463  
 morphology approach, 458  
 movable mirror, 24  
 moving-average filter, 340  
 moving parts, 17  
 multiangle imaging spectroradiometer (MISR), 190  
 multistage VQ, 89  
 multiple-burst bit-error, 150  
 multiple-subcodebook algorithm, 88  
 multiresolution, 254, 448  
 multiresolution analysis, 96  
 multiresolution wavelet, 255  
 multisensor, 244  
 multisource data, 243  
 multispectral, 2, 3, 5, 6, 8–10, 91, 114  
 Multispectral Camera (Mx-T), 10  
 multispectral image, 57, 243  
 multispectral sensor (MSS), 7, 55, 188  
 multivariable, 64  
 multivariate, 251  
 muscovite, 422  
 mutual information, 67
- N**
- N-FINDR algorithm, 419, 444, 458, 459  
 nadir mode, 27  
 nadir-projected area, 32  
 narrow-band indices, 365  
 natural logarithm, 198  
 natural object, 243  
 natural site, 193  
 Nautical Almanac Office, 197  
 navigation satellites, 1  
 near-Earth link, 149  
 near-infrared (NIR), 2, 5–8, 10, 15, 18  
 near-lossless compression, 81  
 near-polar orbit, 34  
 nearest neighbor (NN), 430  
 nearest partition set, 88  
 neighbor-oriented local sum, 116  
 neighborhood, 222, 353  
 neighboring sample, 115  
 nesting effect, 462  
 neural network classifier, 95  
 neural networks, 458  
 neutral density filter, 188, 191  
 Next-Generation Space Telescope (NGST), 29  
 nitrogen deficiency, 366  
 no-compression option, 109  
 no-reference (NR) metrics, 56, 74  
 noise-equivalent change in temperature (NE $\Delta$ T), 198  
 noise-free, 84  
 noise-reduced datacube, 394

noise reduction, 328, 330  
noise variance, 334  
noisy radiance, 383  
nominal altitude, 28  
nominal sum, 412  
nonbinary, 150, 152  
noncontiguous, 154  
nonlinear dimensionality reduction, 429  
nonlinear feature extraction, 429  
nonlinear matched filter, 380  
nonlinear property, 429  
nonlinearity, 185  
nonorthogonal wavelet, 255  
nonpunctured code, 160, 167  
nonshortened code, 152  
nonstationary, 67  
nonuniformity, 222, 295  
nonvegetated target, 365  
normalization, 182, 254  
normalized difference vegetation index (NDVI), 88, 365  
numerical weather prediction, 36

## O

objective image-quality index, 61  
observational data, 130  
ocean currents, 1  
ocean topography, 32  
ocean-color sensor, 194  
octet-aligned, 130  
odd filter, 265  
Offner, 23  
onboard storage capacity, 56  
one-stop shopping, 45  
operating condition, 188  
operating frequency, 278  
operational control field, 140  
operational control field flag, 136  
operational data gateway, 45  
operational products, 47  
optical filter, 14  
optical path difference (OPD), 26

optical sensors, 2  
optical system, 327  
optical filter, 13  
optical-filter-based spectrometer, 15  
optically opaque, 275  
optimal quantization factor, 92  
optimized soil-adjusted vegetation index (OSAVI), 365  
optomechanical, 229  
oracle, 331  
orbital track, 7  
orbiting constellation, 127  
orbiting relay, 127  
organic compounds on Mars, 52  
original image, 56  
orthogonal, 255  
orthogonal directions, 50  
orthogonal subspace, 459, 463  
orthogonal subspace projection, 380, 459  
orthogonal wavelet, 255  
oscillating mirror, 7  
out-of-band spectral rejection, 183  
outer code, 163  
outer Reed–Solomon code, 149, 151  
outlier, 437  
overcompensated, 231  
overhead, 153  
oversampling, 38  
ozone, 27

## P

packet data field, 130, 133  
packet length, 128, 130  
packet order flag, 137  
packet primary header, 130, 131  
packet secondary header, 130, 133  
packet sequence control field, 131, 132  
packet telemetry, 125  
packet type, 132  
packet version number, 131  
packetization layer, 128, 145

- pan-sharpening, 76, 245, 258
- panchromatic, 2, 91
- panchromatic image, 3, 5, 10, 57, 78, 245
- Panchromatic Remote-sensing Instrument for Stereo Mapping (PRISM), 3, 12, 13, 18
- Panum crater, 3
- parallel model, 459
- parallel operation, 89
- PARASOL, 34
- parent-child coefficient relationship, 440
- parent-child relationship, 353
- parity check, 159
- parity-check matrices, 171
- parity symbol, 153
- partial information, 68
- partition, 88
- passive instrument, 274
- passive sensors, 2, 30
- pattern recognition, 261
- payload, 289
- payload design, 291
- peak signal-to-noise ratio (PSNR), 58, 304
- penalty, 437
- penetrate, 275
- penetration depth, 278
- per information bit, 146
- perceived visual quality, 57
- percentage area, 395
- percentage maximum absolute difference (PMAD), 58, 85
- perceptual quality, 68
- periapsis, 36
- permutation, 168
- Phased Array-type L-band Synthetic Aperture Radar (PALSAR), 278
- phases, 328
- photointerpreter, 93
- photon, 84
- photonic effects, 55
- photosynthetic pigment, 364
- phyllosilicates, 22
- piece-wise smooth, 329
- pipeline, 166
- pipeline products, 47
- pitch size, 206
- pixel-level fusion, 244
- pixel purity index (PPI), 434, 439, 458, 461
- Planetary Data System (PDS), 43, 46
- planetary ephemerides, 47
- planetary science, 43
- platform ephemeris, 46
- Pleiades-HR satellite, 93
- point spread function (PSF), 55
- Poisson distribution, 84
- polarization, 183, 278
- pollution fraction, 412
- polynomial, 141, 153
- polytetrafluoroethylene, 188
- polythene, 305
- postcalibration, 196
- postfiltering, 295
- postlaunch calibration, 181, 193
- postprocessing, 15
- preamble field, 134
- predefined fraction value threshold, 405
- prediction, 107
- prediction-based lossless compression, 82
- prediction-based lower triangular transform, 101
- prediction error vector, 99
- prediction residual, 115
- prefiltering, 295
- preprocessing, 419, 459
- preprocessor, 107
- previous spectral bands, 115
- primary header, 128
- principal axes, 352, 420



- principal component analysis (PCA), 251, 328, 349, 419
- principal component analysis fusion, 246
- principal component substitution, 251
- principal components, 352, 420
- principle wavelength, 15
- prior-to-launch calibration, 181
- probabilistic mixture model, 456
- probability, 156
- probability density functions (PDFs), 73
- probability of detection, 389
- probability of false alarm, 389
- product generation, 44
- Project for Onboard Autonomy (PROBA), 20
- projection, 302
- projection onto convex sets, 295
- projection operation, 295
- protocol, 125, 126, 145
- Proximity-1 Space Link Protocol, 127
- pseudo-polar Fourier transform, 262
- punctured code, 160
- punctured encoder, 159
- pure mineral, 422
- pure pixel, 406, 458
- pure signal, 330
- purest pixel, 394, 419
- push-broom, 4, 16, 22, 38, 117, 205
- push-broom imaging spectrometer, 292
- pyramid, 255
- Q**
- $Q$  index, 62, 278
- $q$ -norm, 78
- $Q$ -switched, 33
- $Q4$  index, 62
- qualitative evaluation, 93
- qualitative result, 259
- quality metrics, 55
- quantitative evaluation, 93
- quantitative result, 259
- quantization, 75
- quantization error, 101
- quantization noise, 84
- quantization noise feedback loop, 85
- quantum efficiency, 39
- quantum fluctuation, 84
- quartz halogen lamp, 189
- quasi-cyclic code, 172
- quaternion, 62
- quick look, 153
- QuickBird, 2, 61, 246, 277
- R**
- radar, 2
- radar imaging, 262
- radar sensor, 274
- RADARSAT-1, 277
- radiance data, 84
- Radio Frequency and Modulation Systems, 126
- radio frequency (RF) signal, 126
- radiometric calibration, 50, 84, 179
- radiometric images, 7
- radiometric noise, 55
- radiometric normalization, 291
- radiometric response, 179
- Radon slices, 261, 313
- Radon transform, 261, 262, 313
- Raman lidar, 31
- Raman scattering, 31, 51
- Raman sensor, 51
- Raman shift, 53
- Raman spectra, 52
- random code, 167
- rate-regulation algorithm, 92
- ratio enhancement, 252
- raw instrument data, 45
- Rayleigh channel, 35
- Rayleigh lidar, 31

- Rayleigh scattering, 31  
real time, 70  
real-time processing, 295  
receiver operating characteristic (ROC), 389  
receiver side, 70  
receiving end, 137  
reconstructed image, 82  
reconstruction fidelity, 86  
rectangular interleaving, 154  
rectilinear grid, 206, 292  
recursive convolutional code, 166  
recursive HSOCVQ, 84  
red-edge, 364  
red-edge position, 366, 370  
red-edge range, 366  
reduced ambiguity, 245  
reduced data records, 46  
reduced-prediction mode, 117  
reduced-reference metrics, 56, 68  
redundancy, 81, 421  
redundant wavelet, 255  
Reed–Solomon block-oriented code, 129  
Reed–Solomon code, 147, 150  
Reed–Solomon outer code, 129  
reference band, 234  
reference image, 56  
reference panel, 179  
reflectance contrast, 364  
reflectance data, 84  
reflective light, 2  
region of interest (ROI), 94  
region of non-interest, 94  
register, 159  
regularized reconstruction, 295  
regulation stability, 92  
relative calibration, 181  
relative global error in synthesis, 61  
relative humidity, 27  
relative-mean-square error (ReMSE), 58  
relative radiometric calibration, 181  
reliable, 145  
remote sensing, 3  
remote sensing community, 205  
renormalized difference vegetation index, 365  
replacement, 244  
reservoir, 311  
residual, 83  
residual error, 462  
resolution enhancement, 70  
resolution ratio, 78  
Return Beam Vidicon (RBV), 7  
reversible compression, 81  
RGB color space, 244, 247  
RGB display, 253  
ridgelet, 263  
ridgelet transform, 261, 262, 265  
ringing artifact, 75  
Rogers Dry Lake, Edwards Air Force Base, California, 193  
root-mean-square error (RMSE), 57  
root-mean-square spectral error (RMSSE), 59  
root relative-mean-square error (RReMSE), 58  
rotation, 295  
rotational angle, 307, 406  
rotational misalignment, 237, 294  
rover, 52, 127  
runway, 269
- S**  
Sagnac interferometer, 24, 28  
salt-and-pepper noise, 84  
sample splitting option, 109  
sand, 305  
satellite, 1  
satellite imagery, 1  
satellite mission, 289  
satellite platform, 289  
satellite-data-derived product, 179  
Savitzky–Golay filter, 328  
scalar quantization, 97

- scaling, 295
- scan line, 95
- scanner for radiation budget, 187
- scanning mirror, 233
- scattering, 183
- scattering layers, 32
- scene heterogeneity, 429
- science-data products, 44
- scientific sensors, 145
- SCISAT, 28
- sea-surface temperature, 51
- sea-viewing wide-FOV sensor (SeaWiFS), 187
- search space, 476
- search and rescue, 1
- second-extension option, 110
- secondary header flag, 132
- seed spectrum, 380, 393
- segment, 111
- segment header, 112
- segment-length identifier, 137
- seismic, 262
- seismology, 31
- selective compression, 94
- semantic space, 429
- sensitivity, 187, 291
- sensor calibration, 253
- sensor calibration model, 183
- sensor parameter, 292
- sensor units, 46
- sensors' intrinsic characteristics, 290
- sequence control, 128
- sequence-of-events files, 47
- sequential forward-floating selection (SFFS), 462
- sequential mode, 459
- service interface, 127
- set partitioning in hierarchical trees (SPIHT), 96
- Shannon limit, 148
- shape, 434
- sharpening, 245
- shift invariance, 261, 262
- short-wave infrared (SWIR), 9
- short-wave infrared full-spectrum imager, 216
- shortened code, 152
- shot noise, 84
- shrinkage function, 330
- shutter wheel, 191
- Shuttle Laser Altimeter (SLA), 33
- signal amplitude, 329
- signal deformation, 330
- signal-dependent noise, 327, 329
- signal-domain spectrum, 334
- signal-independent noise, 327
- signal intensity, 84
- signal processing, 2
- signal regularity, 329
- signal variance, 94
- signal-to-noise ratio (SNR), 55, 58
- signed integer, 114
- similarity map, 370
- simplex, 458
- simplex growing algorithm (SGA), 458–460
- simplex volume maximization, 458
- sine, 328
- singularity, 261
- skewer, 461
- sliding window, 68
- slit, 12
- slit curvature, 205
- slope-based indices, 365
- smart compression, 94
- smile, 17, 205
- smoothing effect, 55
- smoothing filtering, 328
- snow cover, 1
- snow/ice cover, 51
- Sobel filter, 232
- Sobel kernel, 232
- soft decision, 162
- soft thresholding, 329, 441

- soil-adjusted vegetation index (SAVI), 365
- solar backscatter, 27
- solar diffuser, 184
- solar diffusion panel, 181
- solar flux, 185
- solar illumination, 32
- solar-radiation-based calibration, 187
- solar sensor, 181
- solar zenith angle, 185, 197
- solid block, 24
- solid state recorder, 9
- sounder, 114
- source packet, 126
- Space Communications Protocol Specifications (SCPS), 126
- Space-Data Link Protocol, 125, 127
- space data network, 125
- space-ground link, 128
- space packet, 130
- Space Packet Protocol, 126, 127, 131
- space-sampling distance, 50
- space-time grid, 46
- space-to-ground link, 126
- space-variant, 67
- spacecraft, 1, 126
- spacecraft command and control, 44
- spacecraft ephemeris, 47
- spacecraft location, 48
- spacecraft's primary coordinate systems, 47
- sparse, 171
- sparse representation, 329
- sparse symmetric matrix, 432, 439
- sparsity, 262
- spatial dimension, 13
- spatial distortion, 17, 56, 208
- spatial distortion index, 77
- spatial domain, 83
- spatial misregistration, 290
- spatial modulation, 24
- spatial neighborhood window, 419, 429, 431
- spatial resolution, 2, 86, 245, 289
- spatial response, 180
- spatial-resolution-enhanced image, 70
- spatial shift, 233
- spatial-spectral endmember extraction, 458
- spatial uniformity, 180
- spatially variable scene, 294
- speckle-reducing filter, 278
- spectral angle (SA), 60, 240, 469
- spectral angle mapper (SAM), 60, 88, 316
- spectral band, 50, 55
- spectral bandwidth, 15
- spectral channels, 95
- spectral correlation (SC), 60
- spectral derivative, 366
- spectral derivative component, 344
- spectral derivative domain, 329, 337
- spectral derivative image, 338
- spectral dimension, 14, 205
- spectral direction, 13
- spectral distortion, 17, 56, 205
- spectral distortion index, 77
- spectral domain, 83, 86
- spectral emissivity, 197
- spectral-feature-based binary code (SFBBC), 87
- spectral features, 212
- spectral integration, 339
- spectral interpretation, 239
- spectral library, 394
- spectral line curvature, 205
- spectral line smile, 206
- spectral matching, 328
- spectral mixture, 456
- spectral modulation, 24
- spectral profile, 86
- spectral radiance unit, 196
- spectral range, 86

- spectral resolution, 86, 289
- spectral response, 179
- spectral response function (SRF), 207
- spectral signature, 85, 379
- spectral signature similarity, 458
- spectral signatures, 261
- spectral similarity measures, 239, 363
- spectral similarity metric, 459, 464
- spectral unmixing, 391
- spectral vector, 57, 86
- Spectralon panel, 192
- spectrograph, 292
- spectrographic imagers (SPIMs), 18
- spectroradiometric calibration
  - assembly, 192
- spectroscopic properties, 53
- spectrum amplitude, 296
- spectrum feature, 89
- spectrum profile, 57
- spectrum variation, 296
- sphere, 181
- Sputnik, 1
- spectral similarity (SSIM) index, 272, 317
- stability, 182
- standard data products, 46
- standard deviation, 218, 249
- standard deviation difference (SDD), 278
- standard products, 43
- standard rule, 145
- standardization, 145
- standards, 106
- static, 136
- stationary, 328
- statistical measures, 363
- steerable pyramid wavelet transform, 74
- Stein's Unbiased Risk Estimator (SURE) threshold, 331
- stochastic geometric model, 456
- straight entrance slit, 206
- stray light, 180, 182–183
- strip-based input formats, 107
- structural distortion measurement, 57
- structural information, 57
- structural similarity (SSIM) index, 65
- subband, 73, 276
- subband image, 110, 254
- subfield, 132
- sublayer, 135
- subpixel, 406, 456
- subpixel shift, 290, 295
- subpixel-shifted images, 294
- subsampling, 87
- substitution method, 244, 246
- subsystem, 126, 145
- successive approximation multi-stage vector quantization (SAMVQ), 89
- sum of fractions, 411
- sum of pollution fractions, 412
- sum of squared error (SSE), 447
- summation, 456
- Sun-synchronous orbit, 28
- sunlight, 455
- super-resolution, 320
- supremum*, 330
- superficies estimation, 381
- superposition, 329
- support vector machine (SVM), 95
- surface albedo, 51
- surface-laid mines, 380
- surface temperature, 96
- surface topography, 38
- surrounding background, 392
- swath, 3, 217
- swath width, 3, 10, 20–23, 38
- symbol synchronizer, 159
- symmetry, 236
- symptom, 231
- synchronization, 127, 135
- synchronization flag, 137
- synchronization frames, 46
- synchronization marker, 93, 128

- syndrome polynomial, 142
  - synergy, 243
  - synonymous, 148
  - synthesis high-pass filter, 98
  - synthesized image, 255
  - synthetic aperture radar, 2, 243
  - synthetic image, 298, 309
  - synthetic object, 243
  - synthetic target, 71, 305
  - synthetic variable ratio (SVR), 246, 252
  - Système Pour l'Observation de la Terre (SPOT), 5, 91
- T**
- TacSat-3, 19, 23
  - target area ratio, 414
  - Target datacube, 305
  - target layout, 307
  - target masks, 392
  - telecommand (TC), 126
  - telecommand packet, 126, 132
  - telemetry, 125
  - telemetry channel, 128
  - telemetry packet, 132
  - telemetry resources, 145
  - telemetry source packet, 128
  - telemetry system, 145
  - telemetry transfer frame, 128, 134
  - telescope, 20
  - temperature, 197
  - temporal coherence, 24
  - terrain, 274
  - terrain roughness, 275
  - terrain topography, 275
  - test image, 56
  - texture, 434
  - Thematic Mapper (TM), 7–9, 188
  - Thematic Mapper calibrator (TMC), 188
  - thermal band, 197
  - thermal infrared, 27
  - thermal noise, 84
  - threshold value, 330
  - thresholding, 232
  - throughput ranges, 15
  - Thuillier spectrum, 197
  - time code field, 134
  - time delay, 24
  - time-division multiplexing (TDM), 126, 129
  - time domain, 24, 328
  - time-ordered sequences, 47
  - time-referenced, 46
  - time reverse, 265
  - time-to-digital converters, 38
  - top-of-atmosphere (TOA), 95, 185
  - top-of-atmosphere reflectance, 195
  - topographic map, 244
  - topological structure, 434
  - trace gases profiles, 96
  - traceability, 180, 187
  - trade-off, 291
  - trained spectral vector, 86
  - transfer frame, 126, 129
  - transfer frame data field, 139
  - transfer frame data field status, 137
  - transfer frame layer, 128, 145
  - transfer frame primary header, 135
  - transfer frame secondary header, 138
  - transfer frame trailer, 135
  - transform-based lossless compression, 83
  - transform coefficient, 102
  - transform kernel, 104
  - transformed chlorophyll absorption in reflectance index (TCARI), 365
  - translation, 295
  - translation-variant, 330
  - transparent, 128, 145
  - transparent code, 151
  - trial simplex, 465, 467
  - trial volume, 459
  - Tropospheric Emission Spectrometer (TES), 27

true positive rate (TPR), 389  
turbo code, 129, 147, 149, 166

## U

ultraspectral, 81  
ultraviolet, 2  
Ultraviolet and Visible Imagers and Spectrographic Imagers (UVISI), 18  
uncertainty, 84, 184  
uncompressed data, 146  
undecimated wavelet shrinkage, 342  
undecimated wavelet-transform-based algorithm, 370  
undecoded information symbol, 156  
undercompensated, 231  
undetected error, 156  
uniform distribution, 84  
uniform interleaving, 154  
uniform scalar quantizer, 85  
unitary vector, 461  
universal codebook, 86  
universal image quality index, 57, 61, 278  
universal threshold, 330  
unknown endmember, 457  
unmixing, 328  
unsigned integer, 114  
unsupervised classification, 261  
unterminated convolutional code, 148  
uplink signal, 44  
upper triangular matrix, 102  
upsampled, 303  
uranium mine, 267, 305  
uranium ore, 305  
user data field, 134  
user support, 44

## V

vacuum chamber, 17, 188  
validation, 179  
validity time, 51

value-added data, 245  
vanishing moment, 98, 343  
variable-length binary codeword, 117  
variable-length codeword, 108  
variable-length data unit, 126  
variable-length transfer frame, 126  
variable-rate coding, 92  
variance of spectral vector, 60  
vector quantization (VQ), 82  
vector-quantization-based lossless, 82  
vegetated target, 365  
vegetation index (VI), 261, 363, 365  
vegetation-dominated site, 332  
vertex component analysis (VCA), 459, 464  
vertical profile, 24, 27  
very large-scale integration (VLSI), 154  
vicarious calibration, 181, 193  
video data, 126  
viewing angle, 50, 86, 292  
viewing field, 57  
vinyl turf mat, 305  
virtual channel (VC), 128, 136  
virtual channel frame count, 137  
virtual channel identifier, 136  
virtual dimensionality (VD), 422, 470  
virtual zero fill, 151  
visible light, 2  
visual communication systems, 70  
visual information fidelity, 67, 304  
visual inspection, 93  
visual near-lossless, 85  
visual perception, 65  
visual quality, 67  
VisuShrink, 356, 362  
Viterbi algorithm, 160  
Viterbi decoder, 151, 160  
Vogelmann indices, 365  
volcanic ash, 1  
Voyager mission, 169

**W**

water cycle, 27  
water stress for vegetation, 183  
water vapor, 27, 219  
waveform, 146  
wavelength, 2  
wavelet, 72  
wavelet-based denoising, 328  
wavelet coefficient, 72, 93, 254  
wavelet cycle-spinning, 264  
wavelet dimensionality reduction, 419  
wavelet image compression module, 93  
wavelet packet coefficient, 448  
wavelet packet, neighbor-shrinking, and PCA (WP+NS+PCA) transform, 448  
wavelet packet transform (WPT), 448  
wavelet packets, 447  
wavelet shrinkage, 329  
wavelet-shrinkage noise-reduction, 329  
wavelet subband, 73, 304  
wavelet thresholding, 328  
wavelet transform (WT), 72, 82, 328, 349  
wavelet-transform-based fusion, 246

weather forecasting, 28, 49  
weather satellites, 1  
weighted sum, 115  
wet biomass, 367  
whisk-broom, 16, 117, 205, 216  
whisk-broom imaging spectrometer, 294  
white noise, 55, 329  
White Sands, New Mexico, 193  
white tarp, 305, 392  
whitened, 421  
Wide-Field Camera (WFC), 35  
wide-sense stationary property, 103  
width in the cross-track direction, 3  
Wiener filter, 356, 360, 362  
wind speed, 51  
word-error rate (WER), 147  
Working Group on Calibration and Validation (WGCV), 197

**Y**

Yellowstone, 117

**Z**

zeroblock option, 109  
zero-crossing, 76  
zero-order linear interpolation, 303  
zoomed image, 307





**Dr. Shen-En Qian** is a senior scientist and technical authority at the Canadian Space Agency. He is an internationally recognized expert in optical spacecraft payloads, space technologies for satellite missions and deep space exploration, remote sensing, satellite image processing and analysis, onboard satellite data compression, data handling, and the enhancement of international spacecraft data standards. He has been working in these areas for 30 years. He holds nine U.S. patents, three European patents, and several pending patents. He is the author of one reference book and chapters in three others. He has published over 100 scientific papers and produced 100 unpublished proprietary technical reports. He is a fellow of SPIE and a senior member of the Institute of Electrical and Electronics Engineers (IEEE).

Dr. Qian received his B.Eng. in industrial electrical automation in 1982, his M.S. in optoelectronics in 1985, and his Ph.D. in telecommunication and electronic systems in 1990. He was the recipient of the Marie Curie Award (European Community International Scientific Cooperation Program). He received the Canadian Government Invention Award for his multiple patents for satellite missions, and he was twice the recipient of the Director Award from the Federal Government of Canada for his outstanding contributions to R&D in space technology and satellite missions.